A three-fingered, touch-sensitive, metrological micro-robotic assembly tool

Marta Torralba[1], DJ Hastings[2], Jeffery D. Thousand[2], Bartosz K. Nowakowski[2], Stuart T. Smith[2]

[1] Centro Universitario de la Defensa, Academia General Militar; Ctra. Huesca s/n, 50090 Zaragoza, Spain.
[2] Center for Precision Metrology, University of North Carolina, Charlotte, NC28223, USA.

Email (corresponding author): *martatg@unizar.es*

Abstract

This article describes a metrological, micro-robotic hand to manipulate and measure micrometer size objects. The presented work demonstrates not only assembly operations, but also positioning control and metrology capability. Sample-tool motion is achieved by a commercial positioning stage, which provides XYZ-displacements to specimens. The designed and manufactured gripper tool that incorporates 21 degrees-of-freedom for independent alignment of actuators, sensors, and three fingers of this hand is presented. These fingers can be opened and closed by piezoelectric transducer (PZT) drivers and flexure mechanisms, i.e. a 80 μm displacement range measured with calibrated opto-interrupter based knife-edge sensors. The attached probes at the finger tips are comprised of quartz 7 μm diameter tuning fork, 3.2 mm long carbon fiber extending from the end of one tuning fork tine. Finger-tip force-sensing is achieved by monitoring of individual finger resonances typically at around 32 kHz. Experimental results included are focused on the probe performance analysis. Pick and place operation using the three fingers is demonstrated with all fingers being oscillated throughout, a capability not possible with the previous single or two finger tweezer type designs. During pick and place operations changes in the response of the three probes demonstrate the ability to identify grab and release operations by monitoring electrical feedback alone. Component metrology has been assessed by contacting three different micro-spheres of diameters 50, 150 and 200 μm. While the deviations in the data are almost comparable to the diameters of the micro-spheres, the three different sizes could be discriminated. This deviation in measured results was primarily due to the manual, joystick-based, contacting of the fingers and difficulties associated with centering the components to the axis of the hand. Finally, micro-assemblies of two spheres onto the edge of a razor blade plus assembly of spherical contact probes for micro coordinate measurement applications are presented.

Keywords: micro-robotic assembly, three-fingered gripper hand, tuning fork probe

1. Introduction

The scale of industrial components is, and has been, shrinking from year to year and processes such as MEMS, microelectronic fabrication processes, and micro-machining tools provide the capability to manufacture micro and even nano-scale components. Complex processes require assemblies produced by a variety of manufacturing techniques. Tools that can select and assemble these components are not readily available or are so highly specialized that they cannot be employed broadly across the manufacturing industry [1,2]. Micro-assembly with dimensional metrology capability is important for the development of micro-manufacturing sensors and actuators. Examples of assembled micro-scale sensors made in our group include micro-metrology [3,4] and indenter instrumentation [5]. More broadly, such a capability is necessary to satisfy demands spanning a broad range of emerging technologies extensively discussed in the reviews of [6] and Bellouard. Other published micro robot system developments are summarized below.

This paper presents a self-sensing, metrological, micro-robotic assembly tool. Key to any such tool is the 'gripper' to grasp and release the components of assembly, in this case comprised by a three fingered 'hand' with the 'fingers' being in the form of 7 μm diameter carbon fibers (the probes) each of which is attached to an oscillator that is used to measure contact interactions. In practice, for small components with major dimensions measuring 10's of micrometers or less, it only requires a single 'finger' to pick up components. For this case, 'grip' relies predominantly on electrostatic or meniscus adhesive forces. In ambient environments, these forces are dependent not only on the current conditions but also the cumulative history of handling of the components and finger usage. However, these fingers are now commercially available and are being used for contact sensing and surface profilometry on ultra-delicate materials and for dimensional measurement, Bauza et al. [3,7,8].

A more positive grip can be achieved with two fingers, a design commonly associated with tweezers. This was previously implemented in our group and used to construct a variety of simple devices. Earlier efforts to measure and assemble micro devices met with a number of unforeseen challenges, these being;

- Cross talk between fibers and feedback signaling.
- Depth of focus issues and depth perception problems using a single camera.
- Because each fiber has similar but slightly different tuning, interphase oscillations would eject the component of assembly during pick-up and release.

In practice, with our two finger gripper design intricate electrical screening was necessary both at the finger location and within the circuit (particularly with the ratio transformers used in the sensing circuits). Manufacturing tolerances result in each probe having similar (within 10's to a few hundred hertz), but distinctly different, operating frequencies. Even using extensive shielding,

the sensitivity of the charge measuring circuits and relatively long signal paths create significant interference problems that have now been largely eliminated with a compact amplifier stage in close proximity to the probe fingers.

While force feedback, dimensional measurement capability, and controlled assembly of micro-devices have previously been demonstrated, there remain a number of fundamental limitations when integrating these capabilities into one, two and three finger micro robot designs. Adhesion forces present themselves throughout the assembly operation. In practice these forces are often time and size dependent with adhesion becoming more of a problem at reduced scale and after prolonged contact. In a typical assembly process, many components will be laid-out on surfaces and transported to the assembly station. Hence, components will have been in contact with a substrate for a relatively long time and, often, have developed a relatively strong adhesion (e.g. adhesion forces due to humidity effects between the object and its original contact surface). This can be overcome by contacting them with an oscillating fiber. In practice, it has been found that when oscillation amplitudes are sufficient to overcome the adhesive forces, the components can be released but are given sufficient energy to launch them with unpredictable speeds in unpredictable directions. This effect is also apparent when one and two-finger grippers are used to determine dimensions of the components, during which oscillation is necessary. Compounding these difficulties, after having been picked up by the gripper, holding the component for significant durations can lead to growth of adhesion forces. Hence, it is generally easier to pick up small objects than it is to place them on a surface. Notwithstanding the above issues, implementation of an oscillating fiber, three fingered gripper has numerous distinct attributes, these being;

- Oscillation of the fibers provides a means of overcoming adhesion forces thereby solving the major problem, at micrometer scales and below, of releasing components from the gripper by activation oscillations of sufficient amplitude.
- Monitoring the electrical work of the tuning fork drive circuits provides an electronic signal for measurement of contact forces and release detection. Consequently, the gripper will be aware of its interaction with the components of assembly.
- Measurement of contact interactions provides haptic feedback capability.
- The gripping fingers can be made from commercially available components and materials that can be scaled to high volume manufacture of single fingers and finger arrays.
- Independent operation of each finger in a compact ‘hand’ design will enable adaptation to accommodate components of different shapes.
- When integrated into metrological positioning stages, detection of contact provides in-situ dimensional measurement capability.

The major advantages of the three finger design that are not possible with other implementations may be summarized as;

- It is demonstrated in this paper that components can be picked up with the gripper finger being active (i.e. with oscillation turned on).
- The gripper fingers can remain active during transport of the components.
- The gripper can perform dimensional measurements of free-standing micro-components.
- For the developed micro robot hand, electronic interference between probes is not significant.

In the following sections the micro-robot developed at the University of North Caroline at Charlotte is presented. First of all, the different parts are described: factory floor, three-fingered hand, and auxiliary devices. After that, the system study analyzes the metrology loop and the probe performance. Regarding the three used tuning forks with matched resonance as nano-probes, experimentation focusses on frequency response and contact sensitivity evaluation of the attached fibers. Finally, the micro-robot performance is discussed in terms of three attributes. These being, the ability to grab and release objects by controlling the amplitude level of the probes. A comparison between measurements of different sizes spheres when being grasped serves to probe the metrology capability. Several micro-assembly operations are presented to illustrate current applications using the robotic system.

As indicated previously, there is a global, industrial push toward miniaturization spanning almost all disciplines to satisfy the need for smaller, faster, lower energy, and less resource hungry solutions. Micro-gripper research around the world utilizes predominantly single probe or two-finger, tweezers-based designs. As far as we are aware, ours is the only group that has used a three finger gripper design and, as yet, no systematic studies for dynamic gripping and control have been published. To conclude, Table 1 provides an overview of current micro-assembly and robotics research activities while additional references can be found in the 2008 WESDA report [2].

Table 1 Summary of global micro-assembly activity

Research group	Major focus areas
Sandia National Laboratory, Precision Micro Assembly Lab.	Probably the most comprehensive micro-assembly facility in the US. Predominantly MEMS based two finger tweezers in broad range of microscopy and clean room facilities with components manufactured using MEMs, LIGA and other processes. Have assembled a micro-robotics work cell. [9]
Harvard Micro-robotics Laboratory	Micro-robotics systems that might be considered biomimetic insect devices. These include flying and crawling mechanisms with major dimension of a few to several centimeters. Design capabilities include; flexure joints, piezo-actuator bimorphs, and memory alloy actuators. Innovations include micro-printing technique that can deposit polymeric and metallic film patterns, meso-scale manufacturing technology. [10–13]
Berkeley Biomimetic Millisystems Lab.	Again, a bio-inspired research group concentrating on design of micro systems for crawling, flying etc. This group also has implemented a two finger tweezer system for assembly. [14,15]
Gracias Laboratories, Johns Hopkins Univ.	Micro and nanoscale assemblies spanning a broad range of applications. At nanometer scales this group has focused on self-assembly mechanisms. [16–18]
Automation and Robotics Research Institute, UT Arlington.	Use a two finger tweezers system in a three dimensional assembly tool for assembly of optoelectronic, MEMS and RF devices. [19–23]
Add Microassembly Inc. and Adept Technologies	Two small business companies company that provide assembly services for RF and custom devices using commercial robotic systems. [24,25]
Zyvex, and Kleindiek Nanotechnik	US and German companies providing single probe and micro tweezers stages for integration into commercial microscopy and robotic systems. [26,27]
Optical tweezers	Optical tweezers using focused beam trapping have been used to arrange and position multiple particles suspended in fluids or air and suspend a single particle for use as a contact probe. Optical tweezers need line of sight and have not demonstrated pick-and-place in the presence of strong adhesion forces or when the objects are proximal to large solid surfaces. [28,29]

2. Principle of operation

The three-fingered micro-robot is designed for the application of pick and place operations. That is assembly of micrometer size components with metrology capability. Hence, two main parts with relative motion define the system, a 3D motion stage that provides positioning of the specimens and a gripper hand. The stationary gripper hand is comprised of three fingers at the ends of which are probes capable of sensing contact with the sample and carrying out the grab and release tasks.

A photograph of the robotic assembly area is shown in Figure 1. It can be divided into different parts described in the next subsections. The factory floor contains the micrometric specimen and its function is to move it along the working volume of several millimeters. The displacements are achieved using a Newport ULTRAlign 561 series XYZ-positioning stage customized with coupled DC motors. The micro-robot hand integrates the three fingers with individual alignment for positioning of the 7 μm diameter fiber tips to be coincident when the fingers are in the 'closed' position, described in more detail in section 2.2.

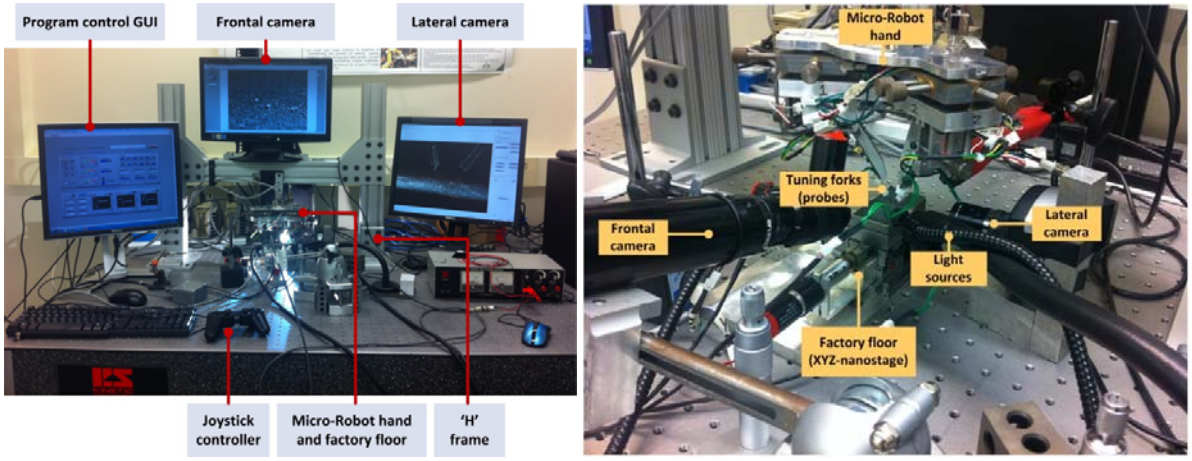

Figure 1: Micro-robot facility: Photograph of the complete facility (left) with a close up image of the assembly area (right).

LabVIEW™ software is used to accomplish the tasks of hardware interfacing, control, and data-logging. All mentioned components are considered in the main project that is individual control algorithms and global implementation. A multi-function joystick is used to control the three axis 'factory floor' stage as well as individual finger motion. For real-time imaging using separated monitors, two high magnification cameras with long range objectives are used to provide visual feedback.

The block diagram of Figure 2 shows a detailed block diagram of the major sub-systems and connections of the complete micro-robot facility. A host PC unit controls the system; moving samples and controlling the three-fingered tool through the DAQ devices. A fine stage and their motor drivers are used for object positioning. The gripper hand with three independent fingers accomplishes the grab and release function. Piezoelectric transducer (PZTs) drivers provide the finger motion as actuators and calibrated opto-sensors measure the finger tip's displacement. The probes are comprised of a quartz tuning fork with a carbon fiber attached to the tine at the free end. Excitation of the tuning fork is achieved by applying a voltage of around 1 V at resonant frequency typically around 32 kHz. Charge used to drive these circuits is monitored using a custom built demodulator, the output of which provides a voltage signal that provides force-sensing operation of the fingers. An auxiliary PC unit monitors the two cameras for real-time visual feedback.

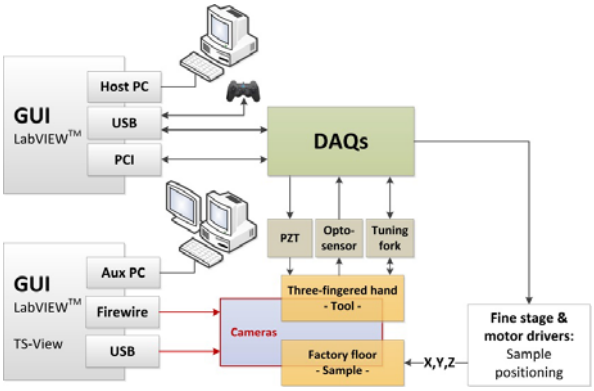

Figure 2: Micro-robot hand assembly: block diagram

2.1. Factory floor

The three axis translation stage used to transfer and position the components of assembly, also called the factory floor, uses a commercial XYZ-stage (Newport, model 561 Series ULTRAlign Stages) with 13 x 6 x 6 mm XYZ-range. Motor driven feed screws translate the factory floor in three axes via a joystick controller with the high magnification, long range objective cameras providing visual feedback. As mentioned previously, the fingers of the hand remain stationary (as also do the cameras) while the platform of the factory floor is used to transfer components to and from the assembly. Given the large number of software functions required for finger sensing, motor controls, electrical signal conditioning for sensors, and motor drive electronics, a substantial effort to reduce delays in all components of this system was necessary to give the user a sense of real time control. In terms of the motor system, it was necessary to assemble these stages with careful motor alignment to reduce stresses in the motor couplings and minimizing mass, as well as isolating electrical current surges from other axis drives. For failsafe operation, using an active-on relay, all motor driver circuits are turned off until the LabVIEW™ global program starts running. Without this safety feature, uncontrolled motor motion can destroy the delicate carbon fiber probe fingers.

2.2. Gripper hand tool

2.2.1. Overall design

Figure 3 shows two models for the three fingered hand. Figure 3 (left) shows a simple model comprising only the essential elements of the hand. This hand comprises a large plate that is the main structure to which all hand components are attached and also has mounting holes to attach to the instrument 'H' frame. This main structure might be thought of as the 'palm' of the hand. Connected to this main frame are three fingers radially aligned at a pitch of 120°. The final design shown in the right part of Figure 3 is the same configuration, but accomplishing manual alignment for the fingers and optical displacement sensors. Alignments are provided using fine adjustment screws with all motions constrained by elaborate flexure mechanisms described shortly. Finite element analysis (FEA) of these aluminum components has been used to ensure that they perform within the elastic limit. Finger displacements are also evaluated for the flexure scheme and to analyze deviations due to the effect of gravity.

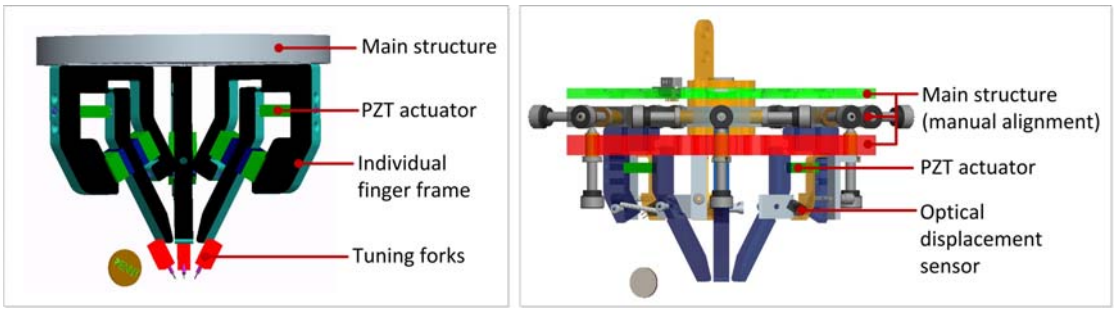

Figure 3: Design of the micro-robot gripper hand (size comparison with a US Penny). Basic hand showing fingers and actuators (left), hand assembled with optical displacement sensors and adjustment mechanisms for alignment of sensors and fiber tips.

2.2.2. Main structure

The main structure supporting the fingers comprises three horizontal metal plates that are rotationally symmetric about the central vertical axis with 120º pitch. These are the support plate, a monolithic flexure and a connection plate. Three different views of this part of the system are shown in Figure 4.

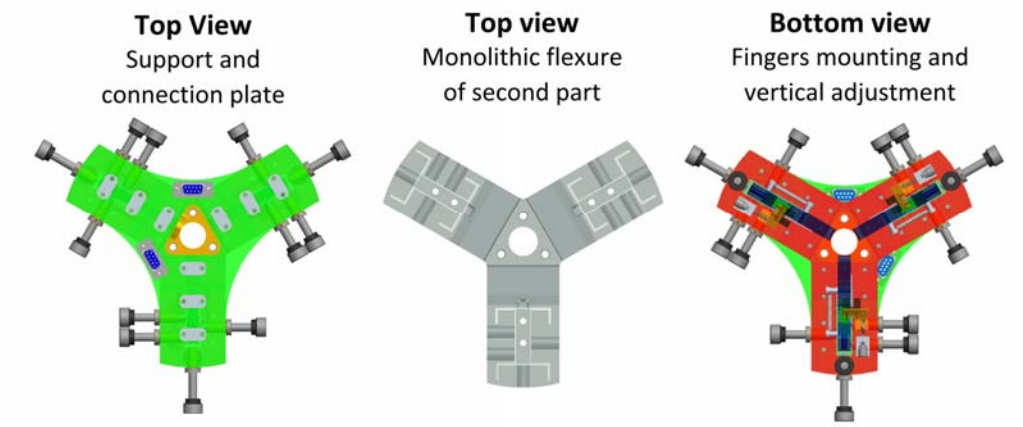

Figure 4: Structure of the gripper hand: solid model design views showing the support plate (green), monolithic flexure (grey) and connection plate (red).

At the top of the hand, the upper support plate of this assembly locates the channels for routing wiring harnesses to two DB9 connectors and supports all gripper components. It is also in this part where the gripper hand is fixed and securely mounted to the horizontal bar of 'H' frame enabling the hand to be positioned vertically above the factory floor. The intermediate plate is a monolithic flexure structure (see Figure 5) that provides fixturing and four axes of adjustment for each finger. This fine manual positioning is achieved in 4-DoF these being; X- and Y-axis, rotational adjustment in the XY-plane, and a vertical adjustment (visible in the right photograph in Figure 5). The third and lower plate incorporates the mountings for independent finger assemblies discussed in the following section. In total, 21 independent alignments are provided by the gripper hand. The plate was designed to attain 250 µm range of linear motion in all three axes with a target alignment resolution of 1-3 µm (operator dependent).

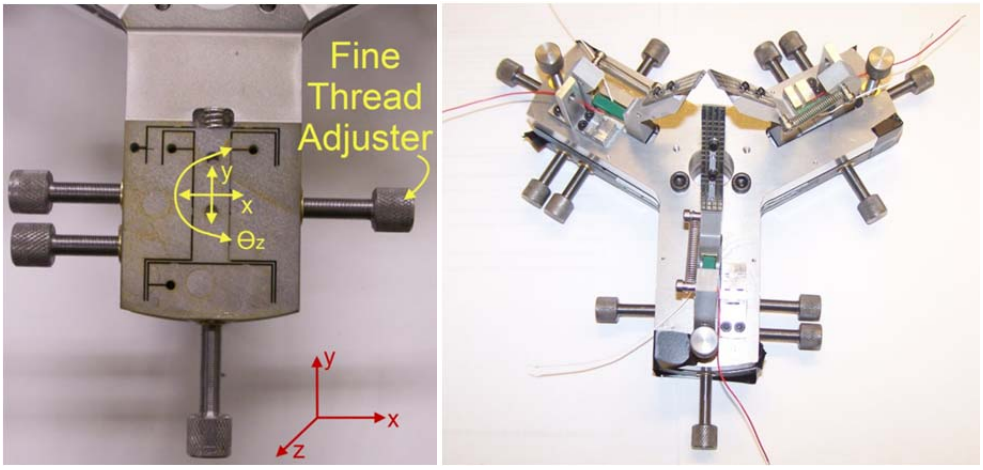

Figure 5 Monolithic flexure intermediate plate and view of the fine threaded adjusters

2.2.3. Independent fingers

Each finger assembly is composed of several components attached to a monolithic flexure, Figure 6. This flexure provides the displacement of a long bar, to which a tuning fork actuated standing wave probe [3] is mounted at the lower, or free, end. The fingers were designed to be coupled with a piezoelectric actuator (PZT) driver. This actuator and its controller (Thorlabs model MDT693A) provides approximately 20 µm of linear motion with a maximum force of 850 N. Due to the distance between the flexure hinge and the PZT, 16 µm displacement at the actuator translates to an amplified displacement of around 80 µm (i.e. a lever ratio of ≈ 5:1) at the tip of the probe.

The motion of the probe is measured by an opto-interrupter [30]. This displacement sensor is based on the changes in the optical intensity as a knife edge attached to the moving finger cuts between a photo diode and phototransistor. The output voltage is translated to distance after calibration of the sensor. This sensor is, in turn, mounted on a slender circuit board that serves as a cantilever flexure to enable manual offset of the sensor, Figure 6. This type of sensor is capable of sub-micrometer resolution over ≈ 100 µm range and represents low cost, easy availability, low added mass, and, consequently, dynamic response.

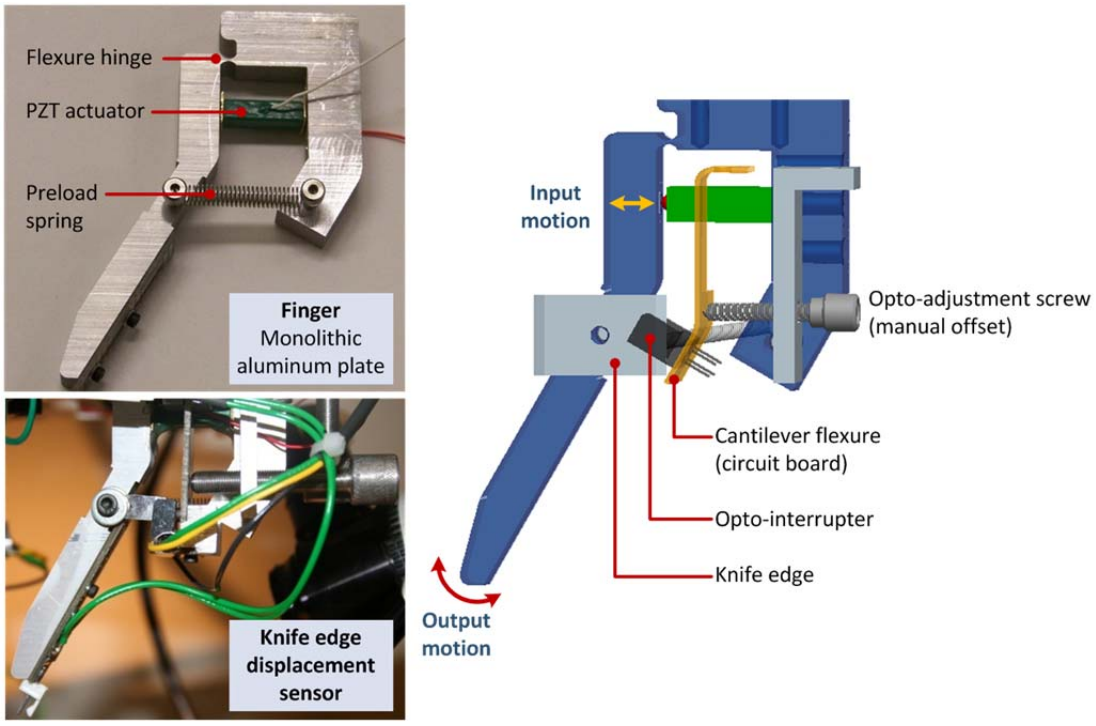

Figure 6 Solid model fingers design; sensor system options and components overview

2.2.4. Tuning fork (probe)

At the end of the fingers shown in section 2.2.3, the probe is constructed of resonant fiber sensors with a 7 µm diameter carbon fiber attached to one tine of a quartz tuning fork oscillator (see Figure 7) [31]. Mechanical resonance of the oscillation is around 32 kHz. The control strategy and design enables easy replacement of probes and frequency response measurement to determine optimal drive frequency that varies from probe to probe. To resolve the probe response, the

frequency of the drive signal to the tuning fork is swept while monitoring the subsequent steady state amplitude and phase in the response. Methods for monitoring the probe responses and sensitivity to contact forces are discussed in section 3.2.

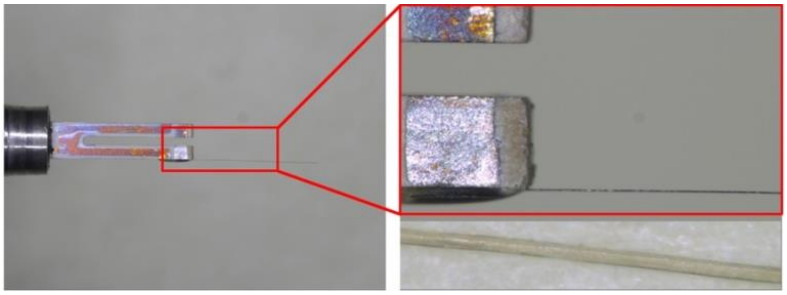

Figure 7 Tuning fork and fiber sensor; the complete probe (left) and a high magnification photograph at the end of the tuning fork tines (right). Below the right image is a photograph of a human hair at the same magnification.

Adjustment of the three probes so that all fiber tips are coincident represents one of the most challenging tasks when assembling the hand. Ideally the three fibers should be aligned to be coincident at one point, symmetrically separated by the same spatial angle. From experience, the following adjustment procedure was determined. With reference to Figure 8, the micro-robot hand was disconnected from the instrument frame and placed upside-down on an auxiliary structure. Individual probes are mounted into Molex® series 6471 connectors and manually mounted to the ends of each finger. The probes are connected so that the fibers form a pyramid with the tuning fork tines oriented away from the pyramid edges, see the lower right image in Figure 8. After that, a manual adjustment was carried out using all available degree-of-freedom of each circuit plate, in view of their screwed mounting of the circuit boards. Final adjustment was achieved using the 21-DoFs of the flexures using two orthogonally placed microscope cameras for feedback.

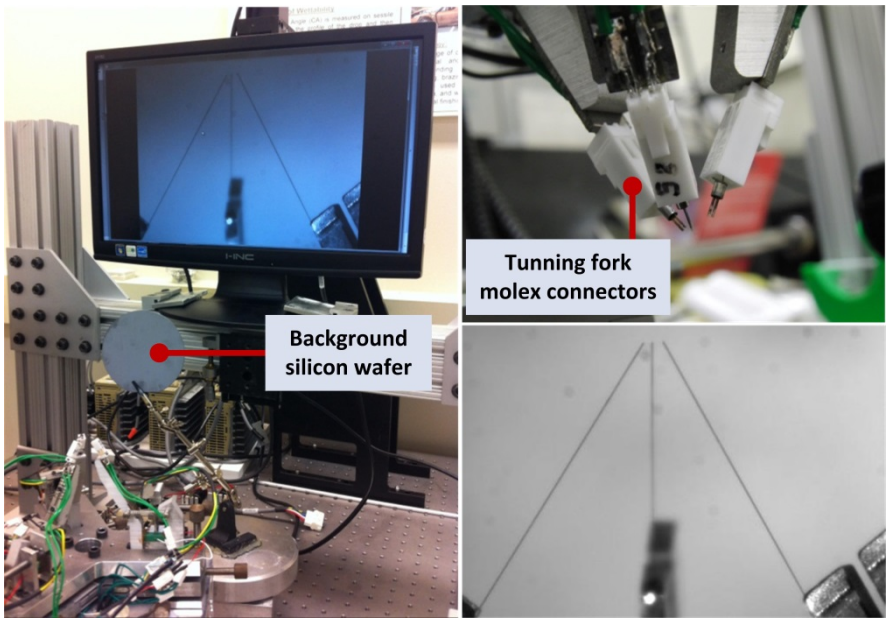

Figure 8 Tuning fork and fiber sensors alignment; upside down hand (left) with a matt finish silicon wafer being used as a diffuse background for lighting, photograph of probes and Molex connectors (upper right), and microscope camera image of the aligned probes (lower right).

2.3. Auxiliary systems

Additional components considered in this section are related to the control task of the tool and include software, the controller, and visual feedback.

2.3.1. Software

The software used for the global control of the micro-robot is National Instruments® LabVIEW™ for which the graphical user interface is shown in Figure 9. Besides the main stop button, the interface is split into four separated blocks:

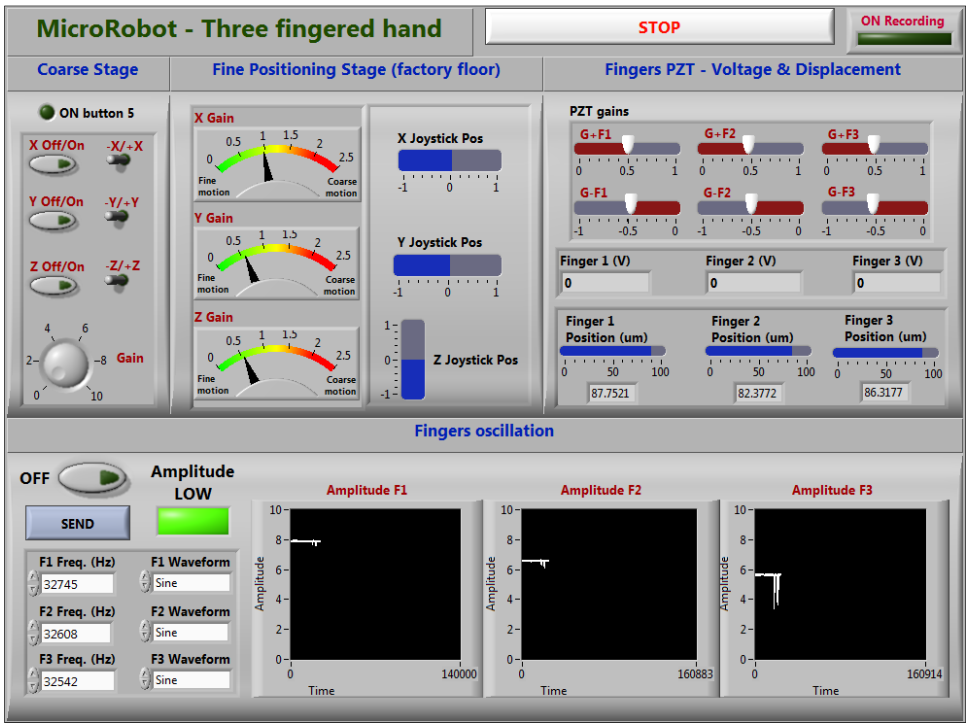

Figure 9 LabVIEW display for the micro-robot control

- **Coarse stage**: not currently implemented, but for control of the long range linear motion in three axes: XY-table and vertical stage, i.e. gain/speed, direction and on/off activation. This will be used to translate the factory floor and hand over longer distances for maintenance of the hand and to remove assemblies or introduce components into the process.
- **Fine positioning stage (factory floor)**: displays the relative joystick position of the controller and provides inputs for defining the gain (i.e. how fast each of the three stages respond to displacement of the joystick paddles) for the 3D-displacements.
- **Fingers PZT – Voltage & Displacement**: manual settings of the piezoelectric finger actuator gains for advancing and retraction, and visual information of the PZT voltage (0-10 V) and opto-interrupter readings (0-100 µm, according to previous calibration).
- **Fingers oscillation**: control of the selected frequency values (Hz) and wave type (sine, triangle and pulse) sent to the three probes. Default options are the resonant frequencies from the previous probe characterization. When changing to a different probe, the send function provides the ability to modify the oscillation parameter and an 'off' button

deactivates oscillation. “Amplitude LOW” indicator shows if the digital switch for the input voltage is high or low (green/red led) that is needed to overcome adhesion forces. Moreover, three amplitude-time charts for each finger are included to visualize sensor responses during operation.

2.3.2. Controller

The user input hardware used in the micro-robot control scheme is a joystick (Etek City gamepad) linked to LabVIEW™. The different functions achieve the control of different operations for the sample and tool. Two joysticks drive the three axis motion of the factory floor and the motion of the fingers with the buttons on the joystick being used to switch between these operations. Other buttons are used to open and close the fingers, and to activate oscillation amplitude inputs to the probes for detection and release operations.

2.3.3. Visual feedback

During micro-assembly operations two cameras enable the operator the view of the sample (e.g. micro spheres) and the ends of the effectors (tuning fork probe tips). Multiple cameras are helpful to provide a three dimensional perspective when aligning the probes and positioning them onto a target or workpiece. One frontal camera (Sony, model XCD-SX910) has been implemented and mounted in an independent structure of the whole system. A specific kinematic base for clamping this device has been manufactured to provide the required DoFs for easily adjustment. It communicates using a FireWire (IEEE 1394) interface bus and the image is displayed in LabVIEW™. This camera also allows the recording of movies during operation. For this reason, and to improve the control loop performance, it was connected to a different auxiliary computer. A second, lower magnification, integrated camera (Ample Scientific TCA-3.0C CMOS model) is connected to the same additional PC unit. The software used in this case to capture images is TS-View.

Images from both cameras are included in Figure 10 to appreciate the two orientations displayed by the software of the working area. In both pictures a dime can be seen next to the probes and over some used spheres to compare the size differences. Light sources are also required for illuminating the working area.

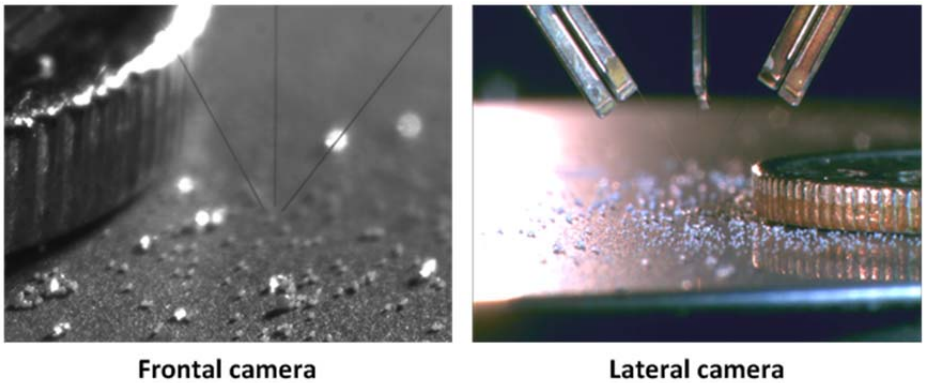

Figure 10: Different camera views: probes, spheres and the edge of a dime for scale comparison

3. System performance

Ultimately, automated micro-assembly operation without human control will depend on the metrological feedback for part measurement identification, and the probe response to determine grip and release dynamics. Thus, this section presents calibration procedures and issues. Additionally, the utility of the tuning fork sensors depends on the signal response when the probe-sample contact takes place during grip and release of components. This section presents experimental results for finger displacement measurement using optical knife-edge sensors and contact response for probe force-sensing.

3.1. Metrology capability of the fingers

The micro-robot integrates three piezoelectric actuators (PZT's) to open and close the finger tips. The knife edge sensor uses an opto-interrupter, whose optical path is partially disturbed by a knife-edge. Prior to assembly it is necessary to calibrate the sensors to relate the output voltage with displacement. Secondly, Abbe error is analyzed, regarding the non-coaxial position between the actuator and the sensor device. Based on experiences during this study, future calibration of finger metrology is evaluated.

3.1.1. Individual optical knife-edge sensor calibration

Calibration of the opto-interrupters has been performed using an Optodyne laser interferometer (Model LDDM), a linear stage, and a data acquisition system. For this experiment, data from the laser interferometer and the output voltage of the metrology circuit are collected during the displacement of the knife edge (manual micrometer) across the interrupter beam path. Results of testing of the finger #1 are shown in Figure 11. Because the knife-edge will translate only around 20 μm, a third order polynomial was used to fit the data over the output range from -6 to 6 V. For this sensor, the residuals represent a deviation of 0.05 V over a 12 V range, or 0.4 %FS. Following this, the geometrically determined lever ratio is used to determinate the actual displacement at the tip of the probe finger (≈ 80 μm).

Due to the difference in position between the metrology circuit and the fiber tip in the measurement loop, an Abbe offset adds uncertainty to the positional measurement of the probes. When the supporting finger pivots about the flexure hinge, the probe tip will follow an arcuate motion that should also be incorporated into the geometric algorithm. Alternatively, to fulfill Abbe's principle and eliminate errors associated with arcuate motion, calibration should occur at the fiber tip (e.g. using a small fiber type laser interferometer for calibration [32]) and be in line with its motion or a more compact sensor might be placed at the tip location. Both of these represent a number of implementation challenges.

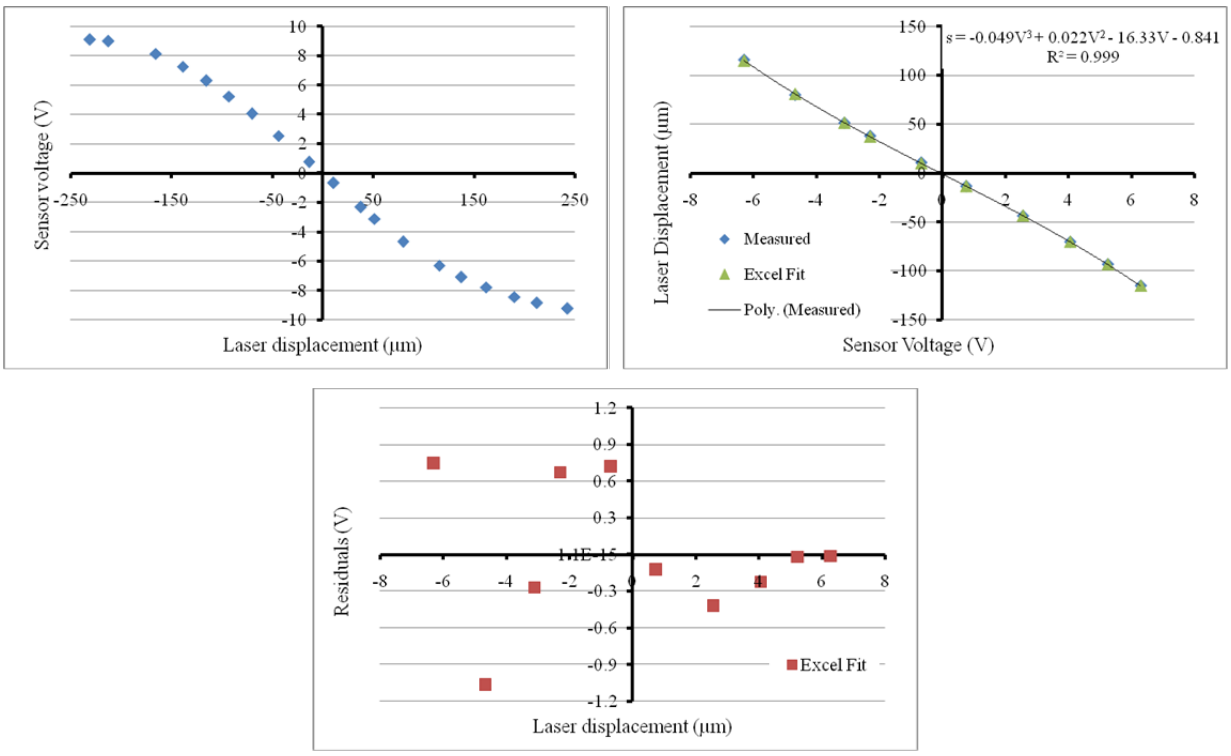

Figure 11 Opto-sensors calibration for finger #1, output voltage over complete range of the sensor (upper left), polynomial fit to the central region of sensitivity (upper right), residuals from the third order polynomial fit (lower)

3.1.2. Micro-robot metrology: considerations

The first aspect to take into account before working with the micro-robot is the necessity of setting the range of the knife edge sensors. That means to relate the range of the PZT actuator (voltage between 0-10 V) and the sensor display (displacements in the range of approx. 10-90 µm). Adjustment to obtain zero output of the knife edge at the mid-position of the PZT actuator is achieved with the cantilever flexure and fine adjustment screw as seen in Figure 6. After this adjustment, the offset and gain of the sensor circuit can be modified to attain the range and offset predicted from the geometric model.

Following adjustment of the sensors, validation of the complete three-fingered tool by studying the metrological micro-robot performance, but with known artifacts (e.g. micro-spheres or pin gages), is necessary. Ideally, this procedure is:

I. Homing of the system: contact probe tips together to set the reference zero.
II. Measuring of known artifacts: to determine lever ratio of sensor to tip motion.
III. Characterization and assembly of components: with the metrology capability of the micro-robot.

Once the system is calibrated, it should be possible to monitor metrological information while picking up and releasing assembly components. Because of the early development and experimental phase of the micro-robot, this procedure has not been evaluated. The goal of this current work is to demonstrate metrology capability by verifying that the displacement knife-edge

sensors can discriminate different sizes of spheres during a grip operation. Initial tests used spheres with diameters between ≈50-200 μm; the results of these studies are in section 4.2.

3.2. Probe response

To obtain touch sensitivity of the fingers, it is first necessary to characterize the frequency response of the probes. For the three fingers, the study of the probe response starts with the frequency analysis of the tuning fork and the glued carbon fiber. From this measurement it is possible to identify the region of the resonance frequency, analyze the signal stability, and demonstrate its change when contact occurs (i.e. touching specimens).

3.2.1. Tuning fork electronics and control

Signal conditioning electronics for independent oscillation and monitoring of all three fiber sensors were developed. A block diagram indicating major components of the sensing electronics for each finger is shown in Figure 12. A Direct Digital Synthesizer (DDS model AD9968) is used to oscillate the fiber at the desired frequency and also to perform frequency sweeps in the probes. Control of all three DDS chips uses bitwise registers sent over a Serial Port Interface (SPI) protocol using a microcontroller (Arduino). Commands are generated in the host program (LabVIEW) and identify the pin number (finger number), wave type (sine, triangle or pulse) and frequency. The oscillation signal is fed to a variable gain amplifier enabling excitation amplitudes between 1 and 5 V prior to being fed to the tuning fork probes through a transformer coupler. The response of the tuning fork is fed to a pre-amplifier (LT1365CN) placed near the robotic hand. A relay switch before the transformer is used to produce a high amplitude signal to overcome adhesion forces when releasing a component.

A relatively low cost signal conditioning circuit is used to extract amplitude using an rms to dc converter (AD637) and phase information. Phase information is extracted by converting the input and response signal to digital form (using an LM311) from which both digital signals then pass through an 'exclusive-or' gate (CD4070). Both of the amplitude and phase signals are then passed through a two pole low pass filter with cut-off at 100 Hz. Voltage changes for the three finger amplitudes are used to detect changes in the signals during operations such as contact with specimens, energizing of oscillation (on and off), and monitoring the release of components.

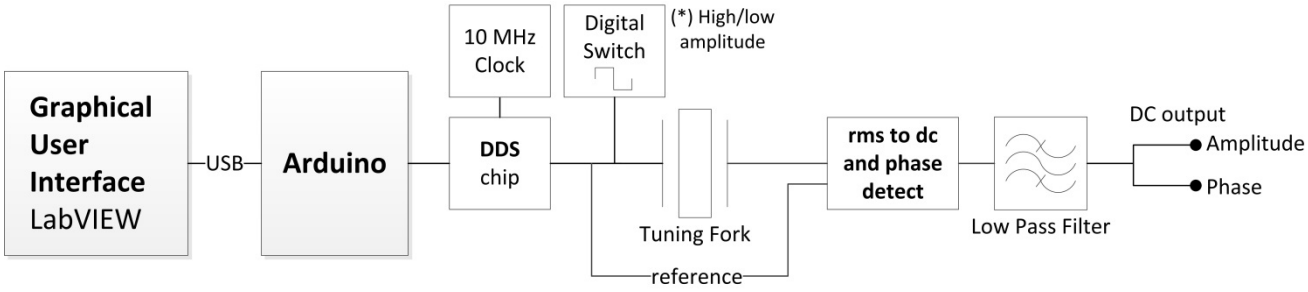

Figure 12 Block diagram of the tuning fork probes signal conditioning electronics.

3.2.2. Frequency response

The quartz tuning fork is an acoustic resonator with a frequency of resonance around 32 kHz. To determine the required value for operation, a frequency sweep is necessary. Therefore, the probe response of the three fingers is displayed and saved in a text file for further analysis. The responses of the three probes used in the studies presented in the paper are shown in Figure 13. When the operating frequency of each separated finger is determined, the digital On/Off switch of Figure 12 is used to activate oscillation at a frequency near to resonance or to deactivate it. The response measurement enables selection of the frequency of oscillation typically at a value slightly below the resonance peak where the contact response tends to be continuous and have lower noise. Once the frequencies for the fingers have been selected, each can be independently activated. Frequency responses are also frequently measured before and after operation to verify that they are operational and discrepancies between response plots is commonly due to particles adhered to the fibers. When this occurs the probes are cleaned by oscillating them in alcohol.

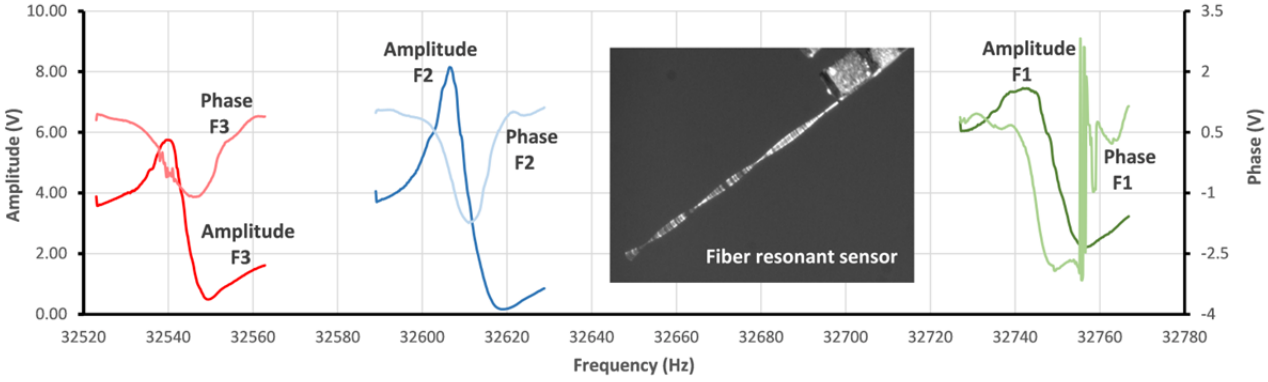

Figure 13 Sweep results of the three fingers for which operating frequencies were 32745 Hz, 32608 Hz, and 32542 Hz for finger numbers 1, 2, and 3 respectively

3.2.3. Contact response

To determine contact sensitivity, changes when the contact occurs should not have less amplitude than the noise range. For this reason, the probe noise is monitored. From Figure 14 a typical peak to valley noise is around 90 mV corresponding to an rms value of around 15 mV. For the probes shown, a typical signal change upon contact with a small glass sphere is around 100 to 200 mV, providing a signal to noise typically greater than 10.

Two contact test were measured. First, the contact response was measured when each finger was contacted against a glass sphere (100-200 μm diameter). Figure 14 shows the change in the signal amplitude of each finger as a function of time after touching a sphere repeatedly. The contact is easily identified in these plots.

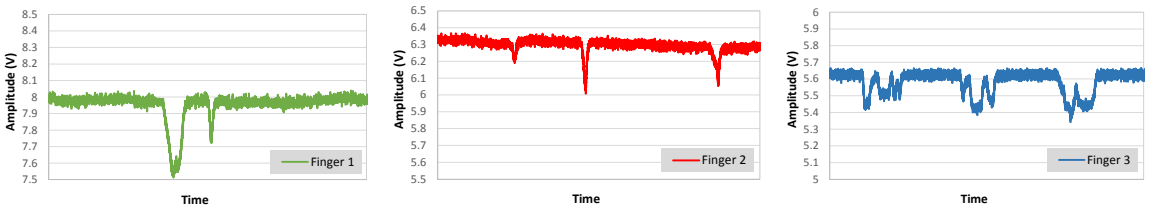

Figure 14 Contact response of the probes: touching a sphere with each finger. There are two contact events in the first plot and three in the other two.

The same test has been carried out by closing the fingers of the hand and displacing the factory floor near to the probe tips. Opening the hand moves the probes in an arc that will bring them into contact with the surface. Figure 15 shows the contact response of the three fingers during three different contact tests, showing repeatable changes in all signals.

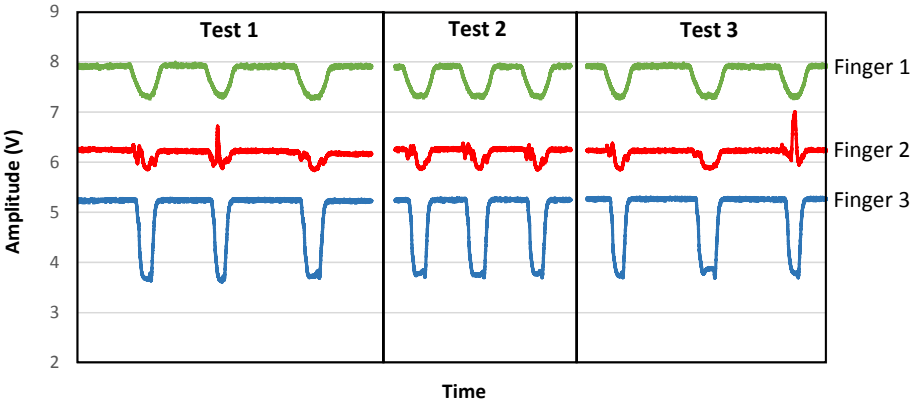

Figure 15 Contact response of the probes: opening fingers and touching surface (all tests)

Based on the above results and experiences when using the hand for assembly, the following conclusions about the contact performance include;

1. In the most cases, the change in the amplitude is significantly above the probe noise, so that the system (probes) is capable of detecting contact.
2. In the most cases, repeating the same test (same kind of contact) produces a similar change in the amplitude signal (in range and form). Then, the change in the amplitude signal when contacting an object is repeatable, if the conditions of the contact test are comparable.
3. Variation in the signal amplitude depends on the test conditions. Differences can appear considering multiple factors. Signal amplitude changes will vary for different operations. For example, contacting a micro-sphere (that is held by significant adhesion forces), or a fixed or a free larger specimen will provide different signal changes. The direction of touching is also significant. Tuning fork probes have a particular direction of vibration, and the fingers and their spatial configuration have an influence. The approaching speed of the probe in all directions is also a factor to take in account, if it is impossible to keep constant in all tests (manual control with the joystick). Different size, material and particle contamination significantly affect the molecular forces between probe and sample at

micrometer scales. Additionally, time plays a factor in the contact response. Over long time periods, moisture from ambient conditions can accumulate on surfaces and adhesion forces change with repeated contact or when in contact for protracted time periods. For example, dust particles that are left on probes for long time periods (hours to days) are considerably more difficult to remove.

4. Initial assembly studies

For this micro-robot system to function as a metrological assembly tool it must be capable of picking up and placing components while being aware of their presence. This section presents studies to validate this performance and is split into three subsections focusing on:

- Pick and place with monitoring and feedback control during the process.
- Discrimination of different size specimens (in this case spheres).
- Micro-assembly examples of stacking of spheres and assembly of a micro CMM-probe.

4.1. Discussion of object grab and release

After probe characterization, the pick-up capability of the micro-robot was studied by monitoring the changes in the amplitude signals while grabbing silica micro spheres. To pick up specimens, the fingers of the hand are retracted from the closed position and located around the sphere. The fingers are then closed and monitored for contact with the specimen. In all of our studies, this is the first time that it has been possible to monitor contact while gripping a specimen. In previous studies, using one and two finger probes, the specimen would be ejected from the finger. This represents a milestone in being able to grip specimens because in the past the adhesion forces between specimen and surface were often greater than that of the fingers making it hard to pick up the part. With the fingers oscillating during the grip operation this difficulty was not observed to be a significant problem. The releasing action has been achieved controlling the input amplitude of the tuning fork with a digital switch. Switching to a high amplitude would ensure release of the sample from the probes. Hence, the pick and release procedure is;

I. Close the fingers and detect the change in the signals when touching the sphere.
II. Pick-up the sphere and move the factory floor to the final sphere location.
III. Activate the high amplitude, open the fingers and release the sphere.

To illustrate some representative results of this, Figure 16 and Figure 17 include two examples of grab and release finger amplitude response with graphs showing signal change in all fingers when touching, the high level in amplitude after activation, and an image of the picked up sphere during the test.

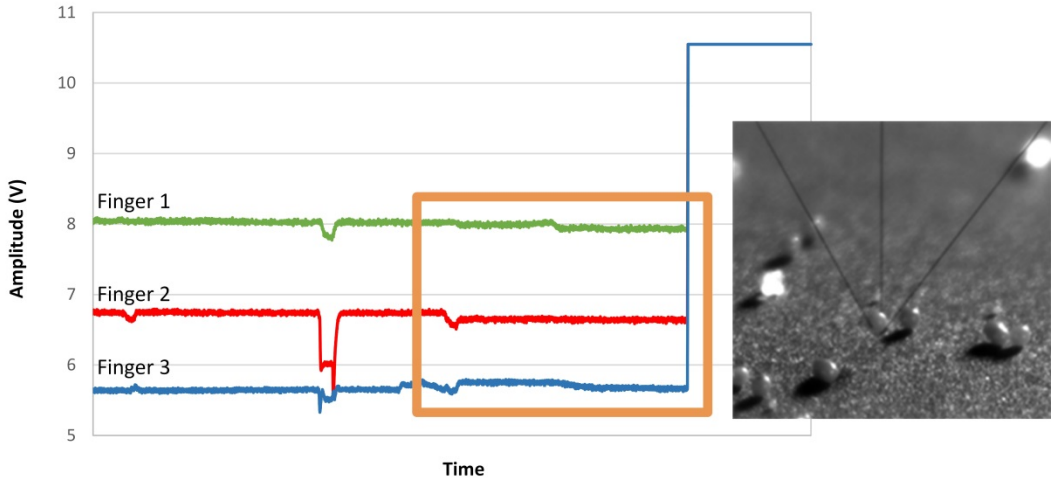

Figure 16 Grab and release experimental results (example 1)

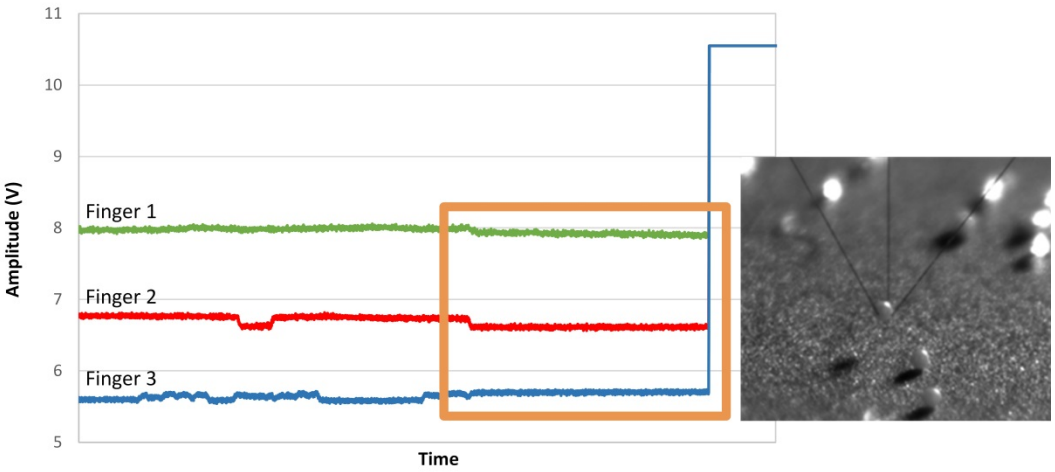

Figure 17 Grab and release experimental results (example 2)

The above examples represent the grab and release operation. This application is possible by monitoring the amplitude response of the three probes and controlling their oscillation amplitude. First of all, by monitoring the change in output signal the ability to determine probe-sample contact is achieved. The interaction between probe-sample and the combination of molecular forces results in the capturing of the sample. After capture, switching on the high amplitude function allows the immediate release of the sphere. The desired place and instant is finally defined by the use of the auxiliary 3D-nanopositioning stage and the two direction long-range objective microscope imaging for visual feedback.

4.2. Discriminating different size spheres

Having the ability to 'feel' contact and measure finger motion, this system is in essence aware of its interaction with components during assembly processes leading to the potential for automated operation without the currently necessary human control. The ability to detect contact and measure the displacements of the fingers provides the ability to discriminate, and ultimately

measure, different size specimens with the three fiber probes. Consequently, this section presents a study to validate metrology applications of the micro-robot hand.

For this study, the diameter of different size spheres has been evaluated to compare if the relative change in this specimen size is related to the relative change in the finger displacement sensor signal, i.e. in the displacement of the probes. The used spheres are shown in Figure 18. Two different materials are used for the different size spheres. Grey microspheres of polyethylene (Cospheric GRYPMS-1.00) are in the range diameters of 45-53 µm and 125-150 µm and glass micro beads (Corpuscular #149119-50) are supplied in batches having diameters between 100-200 µm. To compare the relative change between the size of these spheres and the change in finger displacement, the following procedure was established.

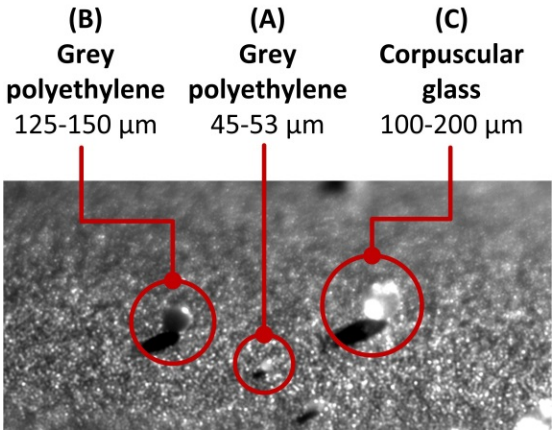

Figure 18 Different sized spheres used to demonstrate the metrology capability

- The sensors are previously calibrated. The change in the voltage is related to displacements after calibration by using a laser interferometer and assumptions about the lever ratio and Abbe lengths.
- There is currently a lack of zero or homing reference for the micro-robot fingers position. In principle, an absolute zero could be achieved by making the three fingers coincident and contacting when the hand is closed.

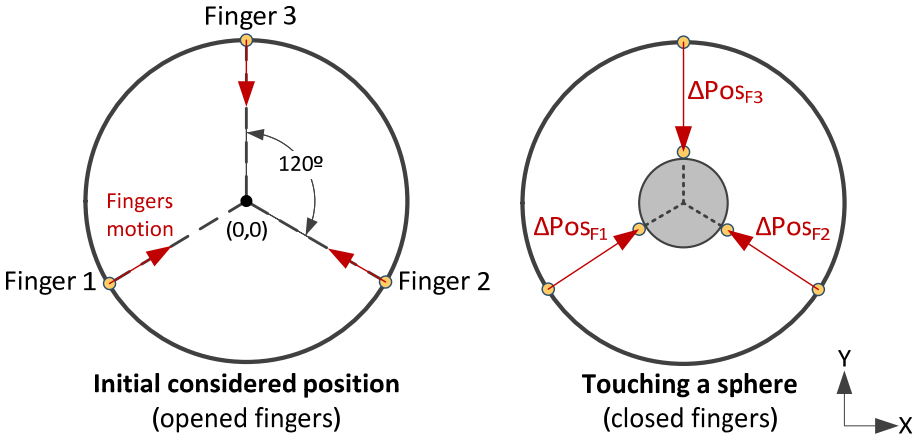

Figure 19 Schematization of the three-fingered model for metrological study

In view of the spheres used, the parameter to calculate is the diameter. Ideally, the three fingers in the initial position and touching spheres are represented in Figure 19. For this geometric model the following assumptions are necessary;

- It is supposed a circular alignment of the three fingers. In other words, they are located over an imaginary circle, in a 120º arrangement and their motion is accomplished along the radial direction.
- The touched sphere is considered perfectly spherical.
- It is supposed that the contact with the sphere is in approximately the central (i.e. equatorial) plane, so that the evaluated distance (displacement of the fingers) is directly related to the diameter of the sphere.

Because only a relative comparison between size of spheres and change in the sensor readings is needed, an absolute zero is not necessary. Thus, the first reading of the sensors with the hand in the 'open' position is considered here as the zero for each finger. Furthermore, the direction of motion is supposed in the XY-plane and defining a straight line for each probe. This approximation is reasonable for the current study despite alignment errors and the arc motion of the tip.

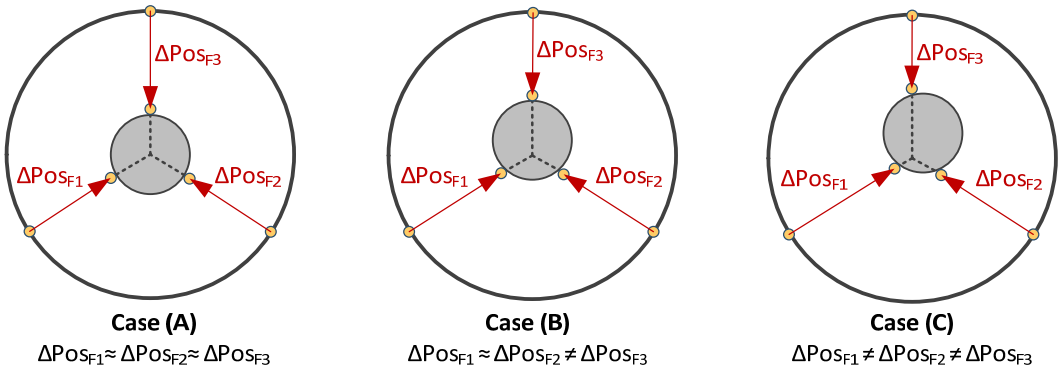

Figure 20 Defined cases to evaluate the diameter of the measured spheres

Figure 19 shows different cases of the probe tips contacting a sphere in the supposed reference system. However, there are three different cases for diameter characterization of spheres (assuming that contacts are about the equatorial line) and the corresponding displacement sensor responses. Figure 20 illustrates these possibilities. In case A, all the obtained displacements are approximately the same value. Case B obtains two measurements with similar values and the other one different. In the last case, case C, all displacements are different. From many experiments it was found that the first case rarely occurs and diameter differences between B and C cases are minimal. For these reasons, all the presented results are considering the mathematical model of case C.

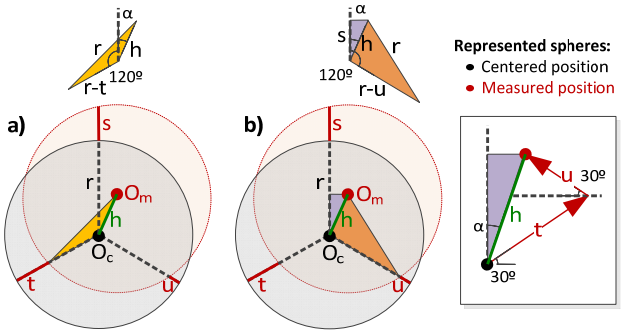

Figure 21 Mathematical model illustration of case (C)

Geometric relations of case C measurements are represented in Figure 21. The hypothetical displacement of the sphere (centered vs. measured position) is characterized by distance h and angle α, obtaining:

$$h = \frac{s}{\cos\alpha} \tag{1}$$

$$\alpha = \tan^{-1}\left[\sqrt{3}\left(\frac{t-u}{t+u}\right)\right] \tag{2}$$

Equations (1) and (2) are a function of the defined parameters s, t, and u; these being the measured displacement differences relative to the center position of the reference sphere ($t > u > s$). That allows calculating the radius of the sphere with two difference geometrical relations:

$$r_a = \frac{h^2 + t^2 + 2ht \cdot \cos(120 + \alpha)}{2h \cdot \cos(120 + \alpha) + 2t} \tag{3}$$

$$r_b = \frac{h^2 + u^2 + 2hu \cdot \cos(120 - \alpha)}{2h \cdot \cos(120 - \alpha) + 2u} \tag{4}$$

Finally, the diameter is calculated as the difference of the considered zero (average of three initial positions i of the n fingers $Pos_{i,n}$) and the average radius:

$$Diameter = 2 \cdot \left[\left(\frac{Pos_{i,1} + Pos_{i,2} + Pos_{i,3}}{3}\right) - \left(\frac{r_a + r_b}{2}\right)\right] \tag{5}$$

With the developed model and after the measurement of the three different spheres, all calculated diameter data is summarized in Table 2. Given the lack of an absolute displacement reference, these values are relative measurements. Finger displacements have been obtained after contact of all three sensors. In these measurements contact has been determined through visually identifying changes in probe signal amplitudes. Such a subjective judgment was found to be operator dependent and repeatability was found to improve with experience. The calculated relative diameters of the different spheres are used to obtain the size relationships between pairs. The purpose is to determine if the ratios agree with those expected based on the diameter range data provided by the manufacturer.

Table 2 Metrology capability results: relative measured diameters

Ball size (µm)	Relative measured diameter of different balls (µm)	Ball size (µm)	Relative measured diameter of different balls (µm)	Ball size (µm)	Relative measured diameter of different balls (µm)
45-53	41.98	125-150	71.89	100-200	87.47
	48.96		75.62		97.25
	63.84		81.91		105.04
*Comment Shaded values are considered not representative for being the limit cases (maximums and minimums).			97.25		105.46
			101.26		107.57
			133.77		110.54
			141.72		152.26
			146.41		162.82

Figure 22 shows a line spanning the expected range for the sphere diameters specified by the manufacturer. Points in the graph are the diameter comparison of each pair of measured spheres. Then, all the results of Table 2 are compared and represented in Figure 22, excluding the shaded values (limit cases). That is for considering only the representative results, eliminating those lowest and highest diameters of each size of balls and the third diameter of the range 45-53 µm, due to the large difference with the other values. As it is shown, the results conclude that the expected ratios agree with the obtained after measuring and treating the data mathematically. Discrepancies appear comparing the more size limited spheres: 45-53 µm and 125-150 µm. That could be justified due to the difficulty of characterization of the smallest spheres. Furthermore, the accuracy of the system is a future issue to address once the measurement loop is properly characterized, out of range of this work.

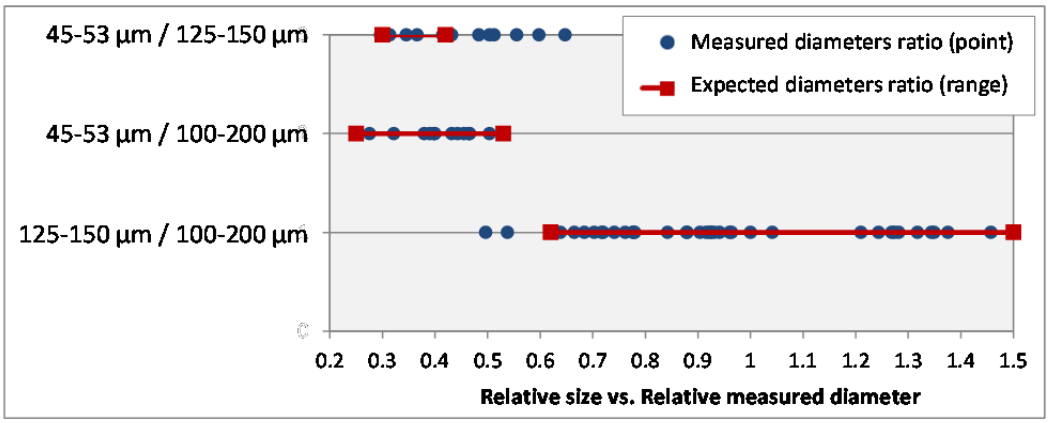

Figure 22 Metrology capability of the micro-robot: relative sphere sizes and measured diameters

This simplified mathematical model when used to calculate the diameter of the sphere, in view of the three finger tips positions validates the relationships between the expected relative change in

the sphere size and the relative change of the measured diameters. While the present system has not implemented an absolute zero or homing for the measurement sensors, the metrology capability of the micro-robot system has been demonstrated, at least for discrimination of the three difference sized spheres of this study. These results compare the relative changes between spheres (possible range of diameters) and the change in the sensor readings.

4.3. Assembly micro CMM: initial studies

Having demonstrated contact detection of the probes, grab and release of components, and metrology capability, this section presented the micro-assembly of contact probes using the micro-robot hand. The following examples illustrate typical pick and place operations. However, it is worthy of note that the first experiments are carried out without using surface proximity sensors. The final example explores the capability of quartz tuning fork oscillator (initiative for indention instrumentation development with nanometer level sensitivity and stability).

4.3.1. Assembly of Ø 30 µm spheres onto razor blade

Figure 23 shows the sequence of steps for the assembly of two glass spheres (30 µm diameters approx.) stacked on top of each other and on the edge of a razor blade. In this case, without the previous sensing of the touched sample (no oscillation of the probes), components are held in place by the naturally occurring adhesion forces between the glass sphere and steel blade in an air environment. Curiously, when attempting to place a third sphere, the stack would fold over resulting in an agglomeration of spheres at the razor blade edge.

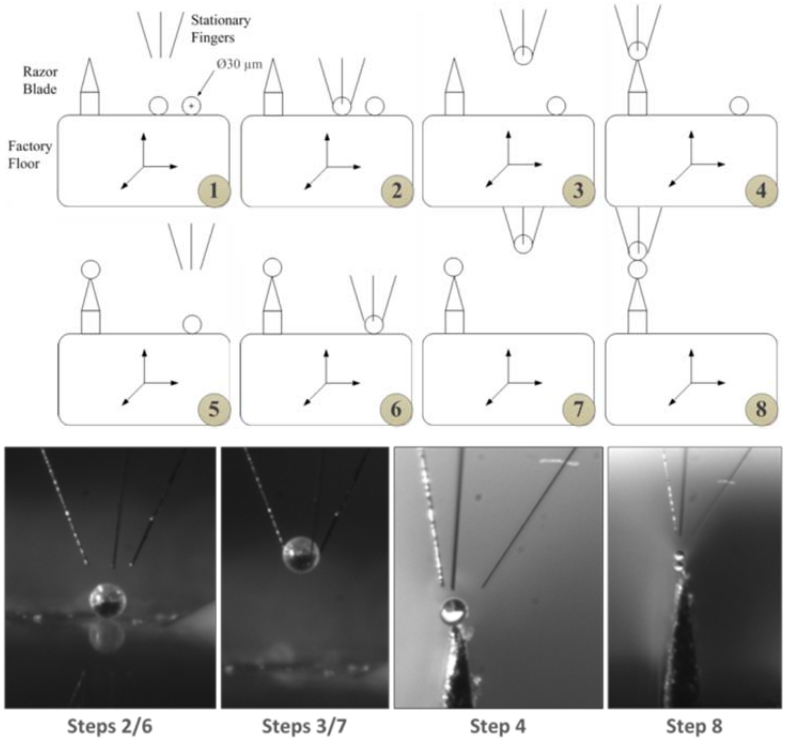

Figure 23 Assembly of two stacked glass spheres mounted onto the edge of a razor blade; Upper figure shows sequence of assembly, lower photographs showing images during assembly.

4.3.2. Attachment of glass spheres to the quartz resonator

Different sizes of glass spheres and types of adhesives were assembled during the experimental study. After each sphere was attached, the quartz resonator was tested by performing a frequency sweep with a lock-in amplifier. The resulting voltage amplitude as a function of excitation frequency was plotted to determine the resonant frequency of the proximity probe, and to evaluate its quality factor. Prior to positioning the sphere with the fine stage, a small amount of glue is deposited onto the tuning fork top tine (with volume being controlled by droplet size and contact time with the tine surface). This globule of glue is attached at the end of a tungsten fiber (75 μm diameter), as shown in Figure 24. After that, the sphere previously selected from the factory floor is then contacted with the glue adhesion forces of which dominate making it easy to release. In some cases the probe fingers are used to apply pressure to the sphere as the glue cures.

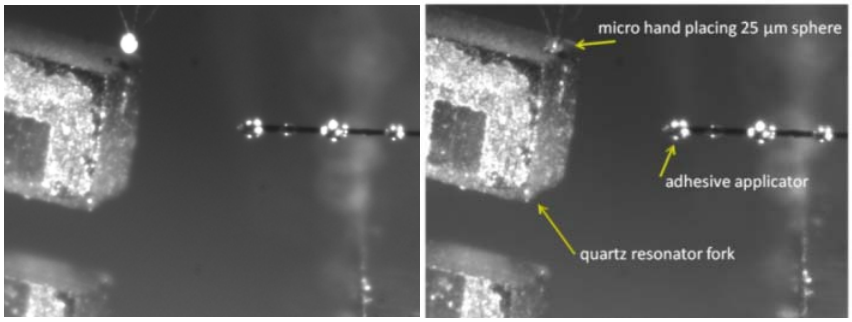

Figure 24 Attachment of a 25 μm glass sphere to the quartz resonator

Following this methodology, different size spheres have been assembled to tuning forks (20 μm to 350 μm, see Figure 25). The aim for the obtained probes is to develop one specific precision proximity nanosensor for position feedback. Figure 25 is a representation of the process for converting a quartz fork to a proximity probe. The fork must be removed from a hermetically sealed can, and to provide a defined contact with the surface of interest, small spheres are to be attached near the tips of the fork. Then, the piezoelectric crystal resonator can be used as a proximity sensor by oscillating it at its resonant frequency. When the resonating crystal is brought close or into contact with a surface, a change in resonance will result. Using a synchronous demodulator, the change in the crystal's resonance can be measured and used to indicate its proximity to a surface.

Smaller sphere sizes resulted in a more symmetric distribution of mass and generally higher quality factor probes. As sphere size decreased the resulting resonant frequency approached the quartz fork's design frequency of 32768 Hz. The best performing probe had 12 μm spheres attached with epoxy. Final testing of the probes was performed in a piezoelectric device with feedback. Those who performed testing of the probes reported that the 12 μm probe had the highest sensitivity. Another assembly of a probe comprising a tuning fork oscillator with an 80 μm fiber attached to the free end of one tine with a 120 μm sphere attached at the free end is shown in Figure 26.

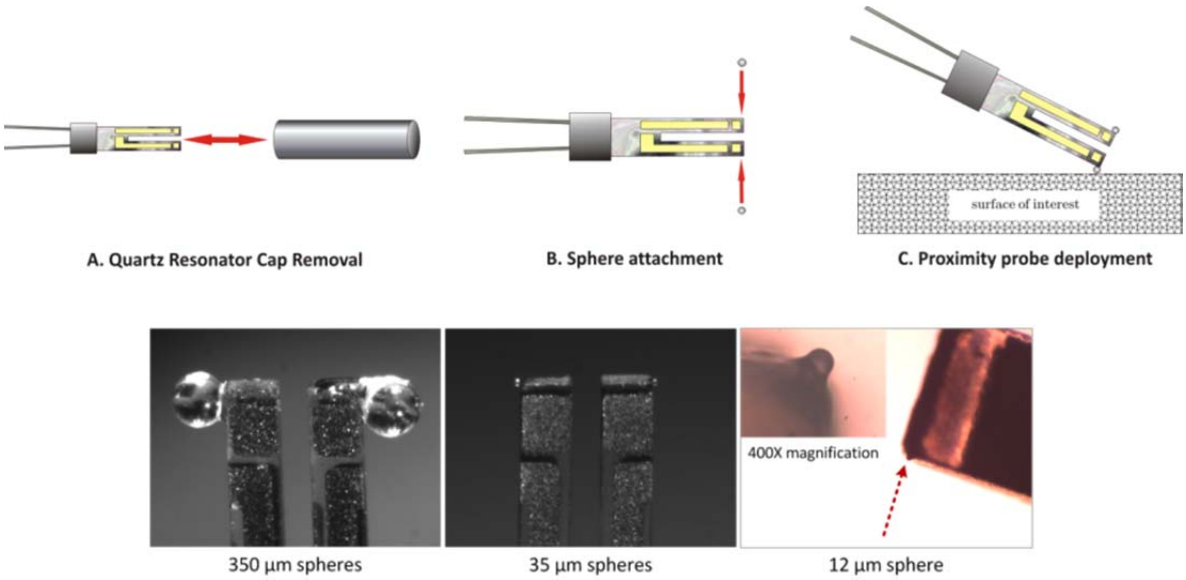

Figure 25 Proximity probe development with the previous micro-assembly task

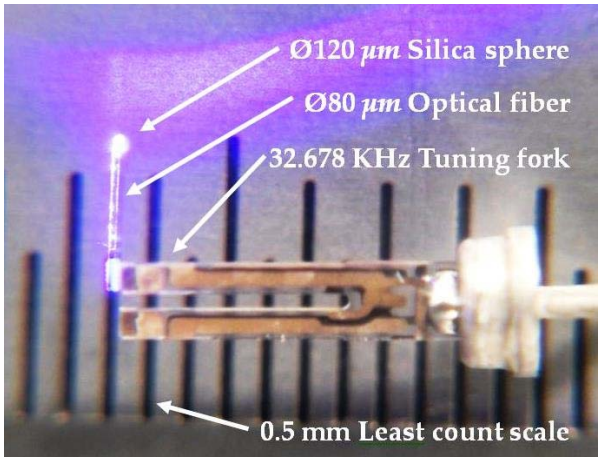

Figure 26 A different probe obtained by the previous micro-assembly task

5. Conclusions

The design and the first experimental results of a micro-robotic hand have been presented. The open architecture of the tool and the micro-positioning capabilities provide a wide variety of applications to manipulate, pick and place, and perform localized metrology on micro-sized objects. The frequency response of the integrated nanoprobes at the end of the three-fingered scheme has been analyzed. The force-sensing capability is possible to achieve after this previous characterization. The demonstrated performance by testing shows the options of these fiber sensors to detect contact. A change in the amplitude is noticeable when the probes reach specimens. The motion in the gripper hand of closing and opening the fingers makes possible to pick-up specimens at micrometer scale. The control in the input amplitude allows controlling the release operation in time and place after grasping. The metrology loop that characterized each individual finger attains the measurement of the finger tips motion. Displacement sensors based on opto-interrupters and a crossing knife edge have been previously calibrated. Their use in the whole

system has been proved that measured results agree with the expected size changes in relative terms. Finally, several micro-assembly examples have been included to illustrate the advantageous operations that could be carried out with future improved prototypes.

Detecting contact for metrology measurements can be automated, thereby eliminating the errors associated with manual joystick control and visual identification of probe tip 'contact'. It is expected that this will reduce the variability found in these early studies.

Experimental studies and use of this tool for assembly of micro devices made apparent a number of potential improvements of this tool. Major among these was the difficulty with alignment of the three fibers so that their tips are coincident and contacting when the fingers are 'closed'. This alignment procedure had to be repeated each time a probe was changed and typically required disconnecting of the hand and turning it upside down to make adjustments more accessible. A complete procedure could take upwards of 4 hours. Another apparent anomaly is the large size of the hand relative to the scale of the assembly operations. Finally, the manufacture of the probes still requires manual assembly followed by a length tuning process to increase finger contact sensitivity. A future design will aim to address these issues.

Finally, while contact sensing does have the potential for haptic feedback, this has not been implemented. Such a feature would provide a tool to learn about the nature of the interaction forces at these scales that are outside of our normal experience at usual scales of manual assembly. From this, it is envisaged that a knowledge base can be developed ultimately to be incorporated into the controls of a more automated assembly tool.

6. Acknowledgments

The authors would like to acknowledge assistance from many colleagues, including John Brien for developing tuning fork oscillator sensing electronics, Johnny Tomlin and Borja de la Maza for assembly of spheres and CMM probes, Jaymes Graham for work on robot hand and electrical circuits, Sajad Kafashi for DDS software routines, Jacob Chesna for software support and implementation insights. Thanks are also due to the Manufacturing Engineering and Advanced Metrology Group (GIFMA) for the sponsoring of the first author.

7. References

[1] Das A N and Stephanou H E 2011 Design of Microassembly through Process Modeling in Virtual Reality *Microtech Conf. expo, Boston, MA, USA*

[2] Ehmann K F, Bourell D, Culpepper M L, Hodgson T J, Kurfess T R, Madou M, Rajurkar K and DeVor R 2007 *Micromanufacturing* (Dordrecht: Springer Netherlands)

[3] Bauza M B, Hocken R J, Smith S T and Woody S C 2005 Development of a virtual probe tip with an application to high aspect ratio microscale features *Rev. Sci. Instrum.* **76** 095112

[4] Seugling R M, Darnell I M, Florando J N, Woody S C, Bauza M and Smith S T 2008 Investigating scaling limits of a fiber based resonant probe for metrology applications *Proceedings of the 23rd Annual Meeting of the American Society for Precision Engineering, ASPE 2008 and the 12th ICPE* pp 120–3

[5] Chesna J W, Smith S T, Hastings D J, de la Maza B, Nowakowski B K and Lin F 2012 Development of a Micro-scale Assembly Facility with a Three Fingered, Self-aware Assembly Tool and Electro-chemical Etching Capabilities *Precision Assembly Technologies and Systems* (Springer) pp 1–8

[6] Nowakowski B K, Smith S T, Mullany B A and Woody S C 2009 Vortex machining: localized surface modification using an oscillating fiber probe *Mach. Sci. Technol.* **13** 561–70

[7] Bauza M B, Woody S C, Seugling R M and Smith S T 2010 Dimensional measurements of ultra delicate materials using micrometrology tactile sensing *Proceedings - ASPE 2010 Annual Meeting* vol 50 pp 73–6

[8] Bauza M B, Woody S C, Woody B A and Smith S T 2011 Surface profilometry of high aspect ratio features *Wear* **271** 519–22

[9] Jones J F, Kast B A and Bailar J M 2005 Human directed assembly of heterogeneous MEMS devices using precision robotics *Proceedings of the 20th Annual ASPE Meeting, ASPE 2005* pp 197–201

[10] Harvard Micro-robotics center, micro.seas.harvard.edu/research.html

[11] Wood R J, Steltz E and Fearing R S 2005 Optimal energy density piezoelectric bending actuators *Sensors Actuators A Phys.* **119** 476–88

[12] Wood R J 2008 Robotic manipulation using an open-architecture industrial arm: A pedagogical overview *IEEE Robot. Autom. Mag.* **15** 17–8

[13] Wood R J, Cho K-J and Hoffman K 2009 A novel multi-axis force sensor for microrobotics applications *Smart Mater. Struct.* **18** 125002

[14] Hoover A M and Fearing R S 2007 Rapidly Prototyped Orthotweezers for Automated Microassembly *Proceedings 2007 IEEE International Conference on Robotics and Automation* (IEEE) pp 812–9

[15] Wood R J, Avadhanula S, Sahai R, Steltz E and Fearing R S 2008 Microrobot Design Using Fiber Reinforced Composites *J. Mech. Des.* **130** 052304

[16] Cho J H, Azam A and Gracias D H 2010 Three dimensional nanofabrication using surface forces *Langmuir* **26** 16534–9

[17] Leong T G, Zarafshar A M and Gracias D H 2010 Three-dimensional fabrication at small size scales *Small* **6** 792–806

[18] Gimi B, Leong T, Gu Z, Yang M, Artemov D, Bhujwalla Z M and Gracias D H 2005 Self-assembled three dimensional radio frequency (RF) shielded containers for cell encapsulation. *Biomed. Microdevices* **7** 341–5

[19] Mayyas M, Zhang P, Lee W H, Popa D and Chiao J C 2009 An active micro joining mechanism for 3D assembly *J. Micromechanics Microengineering* **19** 035012

[20] Popa D O and Stephanou H E 2004 Micro and Mesoscale Robotic Assembly *J. Manuf. Process.* **6** 52–71

[21] Popa D O, Mysorewala M F and Lewis F L 2009 Deployment algorithms and indoor experimental vehicles for studying mobile wireless sensor networks *Int. J. Sens. Networks* **6** 28–43

[22] Popa D O, Murthy R and Das A N 2009 M3-Deterministic, multiscale, multirobot Platform for microsystems packaging: Design and quasi-static precision evaluation *IEEE Trans. Autom. Sci. Eng.* **6** 345–61

[23] Popa D O, Murthy R, Das A N and Stephanou H E 2011 Multiscale Robotics for MicroSystems: Fundamentals of High Yield Micro and Nano Assembly Cells *to be pubished by Springer*

[24] www.addassembly.com

[25] www.adept.com

[26] www.nanotechnik.com/micromanipulators.html

[27] www.zyvex.com

[28] Ashkin A 2000 History of optical trapping and manipulation of small-neutral particle, atoms, and molecules *IEEE J. Sel. Top. Quantum Electron.* **6** 841–56

[29] Eom S I, Takaya Y and Hayashi T 2009 Novel contact probing method using single fiber optical trapping probe *Precis. Eng.* **33** 235–42

[30] Lin F, Smith S T and Hussain G 2012 Optical fiber displacement sensor and its application to tuning fork response measurement *Precis. Eng.* **36** 620–8

[31] Woody S, Nowakowski B, Bauza M and Smith S 2008 Standing wave probes for microassembly *Rev. Sci. Instrum.* **79**

[32] Nowakowski B K, Smith D T and Smith S T Development of a miniature, multichannel, extended Fabry-Perot fiber-optic laser interferometer system for low frequency SI-traceable displacement measurement